Z_2 dependence of the stopping power and the effective charge for MeV helium-ion beams

T. Kaneko
Department of Applied Physics, Okayama University of Science, Ridai-cho 1-1, Okayama 700, Japan
(Received 16 January 1984)

Z_2 (target atomic number) dependence of the electronic stopping powers for MeV helium-ion beams is investigated where the charge-state fractions before emerging from matter play a significant role. The electronic stopping powers for a single helium ion in various charge states and a proton ($S_{\mathrm{He}q+}$, $q=1$ and 2, $S_{\mathrm{H}+}$) are calculated on the basis of Lindhard-Winther theory with the local-electron-density model. The ratio $S_{\mathrm{He}+}/S_{\mathrm{H}+}$ shows the Z_2 oscillation as well as $S_{\mathrm{He}+}$ and $S_{\mathrm{H}+}$. The relation between the effective charge q_{eff} and the mean charge $\bar{q}$ is elucidated in some cases of the incident energy where $q_{\mathrm{eff}} > \bar{q}$ is valid regardless of Z_2 and the q_{eff} values show the oscillatory Z_2 dependence with a small amplitude in contrast with a strong Z_2 oscillation of $\bar{q}$.

I. INTRODUCTION

Since the continuous and intense interest in the slowing-down and charge-changing phenomena developed from early investigations of fission fragments, the stopping powers of matter for an energetic ion have received considerable attention, and the problem of charge-state distributions of the ions penetrating through matter has become a historical problem in atomic collisions in solids. Recently, with the progress of studying fusion plasma as a source of energy supply, these problems occupy an important position in plasma-wall interaction.

So far, a large amount of the experimental data has been compiled on the stopping-power data[1] and on the charge-changing phenomena.[2] Such works enable us to obtain useful empirical expressions both for predicting the energy lost by ions through electronic excitation and the ionization of atoms or free electrons in the target, and for predicting the charge-state distributions of ions in matter or emerging from matter. From a theoretical point of view, some pioneering works[3–5] on the electronic stopping were presented for a point charge intruder within the framework of the perturbation approach.

For heavy-ion intruders, the idea of the effective charge is a useful one to arrange and understand the experimental data and to predict the stopping powers for the ion with no experimental data existing if only the stopping power for a proton in the same material could be obtained. Recently, the electronic stopping powers for a proton and a helium ion were calculated theoretically to produce the Z_2 oscillation, based on treating the ion as a point charge with the effective charge obtained from the experimental data.[6] This shows better agreement with the experimental data than the previous calculation which assumed the helium ion to be completely stripped.[7] In addition, the range of the Z_2 oscillation of the stopping power for 0.4—4.0-MeV helium ions was estimated by taking into account the upper and the lower bounds of the effective projectile charge.[8] The Z_2 oscillation of the stopping power arises from the variation of the electron density in the outer shell and therefore is considered to be characteristic of only the target materials at a given energy of the ion. The effective charge in the slowing-down phenomena is regarded as independent of Z_2 number and depends on Z_1 (the projectile atomic number) and the ion velocity.[1]

On the other hand, recent experiments revealed that the mean charge for backscattered mega-electron-volt helium ions shows the oscillatory Z_2 dependence.[9] The origin of this effect can be explained theoretically by the fact that the electron-capture cross section for a He^{2+} ion has a strongly oscillating Z_2 dependence while the electron-loss cross section for a He^{+} ion shows a monotonical Z_2 dependence.[10] This is supported by the experimental results.[9,11,12] However, the compilation of the stopping-power data for mega-electron-volt helium ions indicates that the effective charge does not depend so strongly on the target elements.[1] The above consideration provokes the problem of how such a behavior of the mean charge of helium-ion beams is connected with the effective charge in the stopping.

Following this motivation, the purpose set up in this paper is (1) to evaluate the electronic stopping power and the effective charge for helium-ion beams by taking into account both the charge-state distribution in matter, where a partially-stripped ion as well as a completely-stripped ion has to be treated; and (2) to understand the relation between the effective charge and the mean charge with respect to Z_2 on the basis of the perturbation theory and the local-electron-density model. In both the experiments and the theories so far, it is common to assume that the charge state is already equilibrated the instant the ions come into matter, and that theories are developed for a single particle with the equilibrated electron distribution bound to it.[13] The procedure developed here is also indispensable and effective to understand the stopping power for preequilibrium heavy-ion beams.[14] In Sec. II the basis of the paper is described as the following: the stopping power for ion beams and the local-density model, the effective charge, and the screening effect. Results and discussions are described in Sec. III, and conclusions are given in Sec. IV. Atomic units are used throughout this paper.

II. BASIS OF CALCULATIONS

A. The stopping power for ion beams and the local-density model

If the particles in every charge state are detected after emerging from matter, the total energy loss per unit length for ion beams, S_{HI}, can be expressed as

$$S_{HI}=\sum_i \phi(i;x)S_i, \quad \sum_i \phi(i;x)=1 , \tag{1}$$

where $\phi(i;x)$ and S_i denote the fraction of the particles in the charge state i at the penetration length x and the stopping power for a single partially-stripped ion (including a fully-stripped one), respectively. The charge-state fraction $\phi(i,x)$ is governed by the well-known balance equation in the charge-changing problem.[2] The measurements of the energy loss have been usually made under the condition of the equilibrated charge state. Then $\phi(i;x)$ should be replaced by the equilibrium charge-state value $\phi(i;x=\infty)$. Here the surface effect is neglected for solid targets. Equation (1) shows that the stopping power for ion beams is obtained by averaging the stopping power for a single particle in all charge states over the charge-state fractions. This equation can be easily derived theoretically from the transport equation of particles. It should be noted that the energy loss accompanied by the charge-changing processes is neglected in Eq. (1). If the particles in a particular charge state are detected, another formula has to be used instead of Eq. (1).[14] Hereafter the velocity or energy region is considered where only the so-called electronic part plays the dominant role in the stopping.

Free-electron gas theory, which was first discussed in detail by Lindhard and Winther[5] for a point-charge intruder and extended for a partially-stripped ion thereafter,[15] allows us to calculate the electronic stopping power as follows:

$$S_i=\int_0^\infty d\omega\,\omega \int_{\omega/v}^\infty dk\frac{1}{k}(8N/\omega_p^2 v^2) \times |Z_1-\rho_i(k)|^2 \mathrm{Im}[1/\epsilon(k,\omega)] , \tag{2}$$

where N, v, ω_p, and $\epsilon(k,\omega)$ are the number density of free electrons, the velocity of the projectile, the plasma frequency, and the dielectric function of a material, respectively. Here the spatial electron distribution $\rho_i(r)$ bound to an ion is assumed to be spherically symmetric so its Fourier transform $\rho(k)$ is spherically symmetric. For helium-ion cases, we take

$$\rho_i(r)=|\psi(r)|^2 N_e ,$$
$$\psi(r)=(\pi a_1^3)^{-1/2}\exp(-r/a_1) ,$$

where N_e is the number of electrons in the ion. The analytical expression for $\epsilon(k,\omega)$ was given in Ref. 5. It is a well-known fact that the energy loss is contributed both from the electron-hole pair excitation branch and from the plasma (resonance) excitation branch. The stopping power from the pair excitation branch is estimated by numerical integration over $(k-\omega)$ or $(z-u)$ space (Ref. 5). As to the estimation of S_i from the plasma branch, the following expression is adopted:

$$\mathrm{Im}[1/\epsilon(z,u)]=-(\pi/2)(\chi^2/3z^2\alpha^{1/2})\delta(u-\alpha^{1/2}) , \tag{3}$$
$$\alpha=z^2+(\chi^2/3z^2)+\tfrac{3}{5} .$$

Then Eq. (2) is reduced to

$$S_i=(4\pi N/v^2)\int_{z_L}^{z_U}(dk/k)|Z_1-\rho_i(2k_f z)|^2 , \tag{4}$$

where

$$z_L=[0.5((v/v_f)^2-(\tfrac{3}{5}) -\{[(v/v_f)^2-(\tfrac{3}{5})]^2-(4\chi^2/3)\}^{1/2})]^{1/2} , \tag{5}$$
$$z_U=C\chi/3^{1/2}, \quad \chi^2=1/(\pi v_f) .$$

The upper limit z_U should be determined as satisfying the condition that the sum of the stopping power both from the pair excitation branch and from the plasma excitation branch is connected continuously with the high-velocity-limit formula. This was confirmed within a difference of a few percents in the case of $C\sim 1.0$, where He^{2+} and C^{6+} ions collide with a carbon target ($r_s=1.66$).

As far as the charge-state fractions are concerned, the balance equation should be solved. However, to include all of the charge-changing branches into the theory is a complicated task except for treating a few charge states[10,16] since we have to discuss the many-body problems for targets with many electrons. And since we want to directly see to what extent the oscillatory $\bar{q}$ values can reproduce the Z_2 dependence of q_{eff} values, we overcome this problem by using the measured charge-state fractions which can be regarded as being equilibrated whether they are measured with the backscattering method or the transmission method.

As for a proton, there are so far no findings of the oscillatory Z_2 dependence of the mean charge from the theoretical and the experimental points of view in the velocity region considered here. It has been insisted that a proton cannot have a stable bound state at any velocity in solids because of the screening effect due to the conduction electrons.[17] Another opinion is that there exists an example in which the calculation of the neutral fraction of a proton beam can show good agreement with the data in the case of a carbon target by using the electron-capture and electron-loss cross sections in the gaseous phase.[18] This may suggest that even in a solid a proton has a "bound state" whose lifetime is no longer infinite. On the other hand, in gaseous targets a proton has at least one stable bound state. However, there is a small percent of the neutral fraction at $v\gtrsim 3v_0$ (v_0 is the Bohr velocity) in the $Z_1=1$ beam.[17] As a result, hydrogen atoms are not assumed to exist in the calculated results shown later. The formula (1) is valid in any case whichever material is used, a solid or a gaseous target.

The local-density models are needed to produce the Z_2 dependence of the stopping power for a proton intruder. In this paper two kinds of local-density models are adopted to describe the spatial distribution of the target electrons. One is for the neutral free atom (atomic picture) and the other is for the solid target (solid picture). When we take the local density $\rho(r)$, the physical quantities used here can be introduced through $\rho(r)$ instead of a constant electron density such as

$$\omega_p(r)=[4\pi\rho(r)]^{1/2} .$$

For neutral atoms, the local density is given by the Hartree-Fock wave functions expressed in terms of the linear combination of the atomic orbitals (LCAO). For solid targets, it is a little bit complicated to describe $\rho(r)$ as precisely as possible. Therefore the simple model is taken,[6] which is appropriate for solids having the well-defined plasma frequency, such as

$$\begin{aligned}&\rho(r)=\rho_0 \quad (R_0>r>R_c)\\ &\rho(r)=\rho_{\text{in}}(r) \quad (0<r<R_c)\end{aligned} \tag{6}$$

where $4\pi R_0^3/3$ corresponds to the occupied volume per atom in a solid and R_c denotes the boundary radius between the outer region and the inner region of an atom. The constant ρ_0 denotes the density in the outer region, which can give the measured bulk plasma frequency. In our case, the Hartree-Fock wave functions are used to determine $\rho_{\text{in}}(r)$ on the basis of conserving the total electron density per atom.

B. The effective charge for ion beams

The effective-charge theory presented up to date for a charged particle is based on the Z_1^2 scaling predicted by both the Bethe-Bloch and Lindhard-Winther theories in the lowest perturbation, apart from the higher-order corrections as in the Z_1^3 or Z_1^4 term. The effective charge for a heavy-ion beam with the atomic number Z_1 is defined by the square root of the ratio of the stopping power for the ion S_{ZI} to that for a proton S_{H^+}, such as

$$q_{\text{eff}}^{ZI}=(S_{ZI}/S_{\text{H}^+})^{1/2} , \tag{7}$$

where a proton beam does not include any hydrogen atoms during its passage. Therefore S_{H^+} is the theoretical stopping power for a proton or the stopping power measured so ideally. S_{ZI} is given by Eq. (1). For the $Z_1=1$ beam

$$q_{\text{eff}}^{\text{H}}=[(\phi_{\text{H}^0}S_{\text{H}^0}+\phi_{\text{H}^+}S_{\text{H}^+})/S_{\text{H}^+}]^{1/2} , \tag{8}$$

and for the $Z_1=2$ beam

$$q_{\text{eff}}^{\text{He}}=[(\phi_{\text{He}^0}S_{\text{He}^0}+\phi_{\text{He}^+}S_{\text{He}^+}+\phi_{\text{He}^{2+}}S_{\text{He}^{2+}})/S_{\text{H}^+}]^{1/2}, \tag{9}$$

where ϕ_A and S_A ($A=\text{H}^0,\text{H}^+,\text{He}^0,\text{He}^+,\text{He}^{2+}$) are the fraction and the stopping power for a particle A, respectively. In the above the case is considered where the negative-charge components can be neglected.

In order to compare the theoretical results with the experimental ones, let us consider the quantity Q, which is defined by the square root of the ratio of the measured stopping power S_{ZI}^* for the Z_1 beam to that for $Z_1=1$ beam S_1^*, such as

$$\begin{aligned}Q&=(S_{ZI}^*/S_1^*)^{1/2}=(S_{ZI}^*/S_{\text{H}^+})^{1/2}/(S_1^*/S_{\text{H}^+})^{1/2}\\ &=q_{\text{eff}}^{ZI}/q_{\text{eff}}^{H} .\end{aligned} \tag{10}$$

This means that Q yields the ratio of the effective charge of the Z_1 beam to that of the proton beam. Therefore in the high-velocity region where any hydrogen atoms can not be incorporated in the beam during the passage being considered, q_{eff}^{H} is regarded as unity and as a result Q is equal to q_{eff}^{ZI}. At the energies considered later (200, 250, and 400 keV/amu), this situation will be satisfied. At the lower velocities, if possible, the fact that q_{eff}^{H} is less than unity plays an important role in estimating the q_{eff}^{ZI} values, especially for gaseous targets.

C. The screening effect

If the ion with the charge Z_1 moves at the velocity $v \ll v_F$ (v_f is the Fermi velocity), the spherically symmetric polarization of the media is induced that screens the electric potential of the ion.[15,17] This potential in the Thomas-Fermi model of a degenerated electron gas is expressed as

$$V(r)=-Z_1\exp(-k_c r)/r \tag{11}$$

as a function of the distance from the ion r within the framework of the random-phase approximation. In the above, the inverse screening length k_c is given by $k_c=(12/\pi)^{1/3}/r_s^{1/2}$, where r_s denotes the radius occupied by one electron in a solid. For the moving ion at the velocity $v>v_f$, the induced polarization of the media becomes asymmetric and, moreover, the screened potential of the ion has the velocity dependence such as

$$V(r)=-(Z_1/r)\exp[-k_c r F(v/v_f)] , \tag{12}$$

where F is a function of v/v_f and $F\sim 0.6$ if $v/v_f=2.0$.[17] This suggests that with the increase of v, the screening effect tends to diminish since the conduction electrons cannot respond to the external charge so rapidly. In our case, owing to including the screening effect partly as simply as possible and partly as strongly as possible into the theory, the static-limit form of the screened potential as shown in (11) is adopted without regard to the ion velocity considered later. The expectation value of the energy of an electron in the ground state, described by the wave function $\psi(r)=(\pi a_1^3)^{-1/2}\exp(-r/a_1)$, of the ion with Z_1, is given by

$$\langle E\rangle=(2a_1^2)^{-1}-(Z_1/a_1)(1+a_1k_c/2)^{-2} . \tag{13}$$

From the condition of the energy minimum $\partial\langle E\rangle/\partial a_1=0$, a_1 can be determined as a function of k_c or r_s. The estimated values a_1 are tabulated in Table I.

TABLE I. Calculated values of a_1 for various solids.

Element	N_f[a]	r_s	a_1 (a.u.)
$_4$Be	2	1.885	0.595
$_6$C	4	1.660	0.609
$_{13}$Al	3	2.075	0.586
$_{14}$Si	4	2.008	0.589
$_{20}$Ca	2	3.421	0.552
$_{31}$Ga	3	2.192	0.581
$_{49}$In	3	2.411	0.573
$_{50}$Sn	4	2.218	0.580

[a]The number of free electrons per atom [D. Pines, *Elementary Excitations in Solids* (Benjamin, New York, 1964)].

As a result, if the above approach is applied to a He^+ ion, the distribution width of the electron orbital a_1 gets a greater value in a solid due to the polarization of the media than $0.5a_0$ (a_0 is the Bohr radius) in a vacuum. This affects the electronic stopping power of the media through the external charge in the Fourier space $|Z_1-\rho_i(k)|^2$. Consequently, the difference between a solid and a gaseous target in the stopping power and also in the effective charge comes from the screening effect through a_1 and from the variation of the local electron density in a target media.

III. RESULTS AND DISCUSSIONS

First, the stopping power for a 200-keV/amu proton moving into various Z_2 materials calculated with the local-density model in the atomic and solid pictures are shown in Fig. 1. The stopping power from the plasma branch presents the oscillatory structure with a small amplitude superimposed on the constant value. On the other hand, the stopping power from the pair excitation branch has the same oscillatory Z_2 dependence with a greater amplitude superimposed on the monotonical increase with respect to Z_2. Except that the overall values of the total stopping power seem to be less than the experimental data[19–24] especially in the high-Z_2 region, they can reproduce the well-known Z_2 oscillation. This is due to the nonmonotonical variation of the valence electron density. Some examples, i.e., Be, C, Al, Si, Ca, Ga, In, and Sn, of the calculation in the solid picture show the improvement of the deviation between the experimental results and theoretical ones.

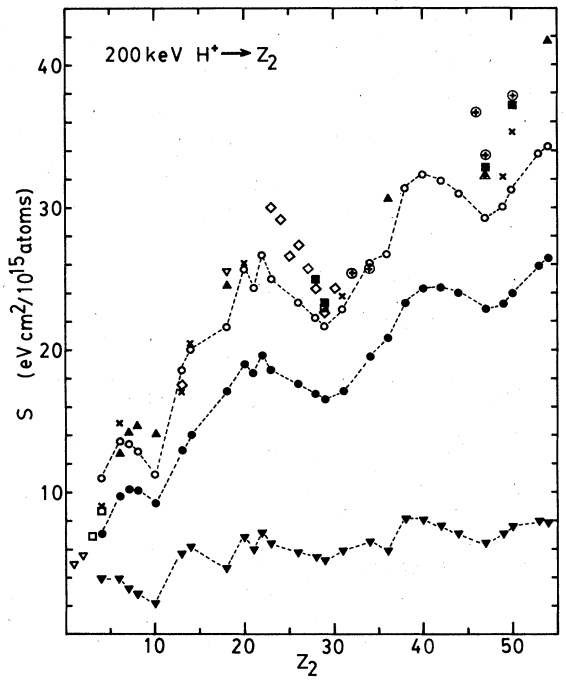

FIG. 1. Z_2 dependence of the electronic stopping power S_{H^+} for 200-keV/amu protons. Theoretical results denoted by (– – –▼– – –), (– – –●– – –), and (– – –○– – –) are the stopping powers from the plasma branch, from the electron-hole pair excitation branch, and the total stopping powers, respectively, in the atomic picture. The crosses (×) denote the total stopping powers in the solid picture. The other symbols denote the experimental results: ▽—Ref. 19; □◇—Ref. 20; ■—Ref. 21; ▲—Ref. 22; ⊕—Ref. 23; ⩓—Ref. 24.

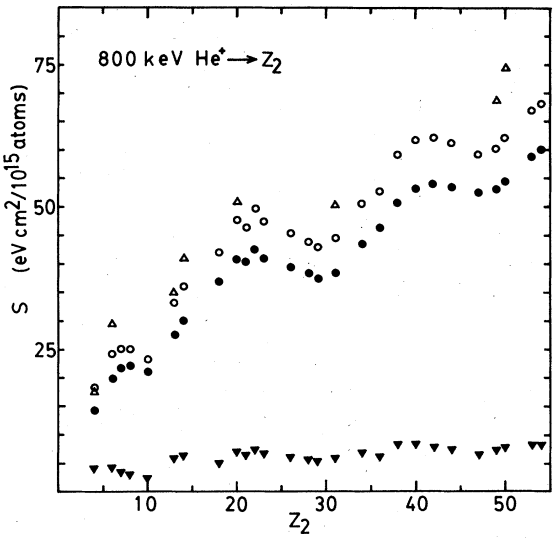

FIG. 2. Z_2 dependence of the electronic stopping power S_{He^+} for 200-keV/amu He^+ ions. The symbols (△) denote the total stopping powers in the solid picture. For other symbols, see Fig. 1.

Figure 2 shows the calculated stopping power for a He^+ ion with the local-density models. The contribution of the plasma branch is not so different from that for a proton at the same velocity, as is clear in comparison with Fig. 1. This is because only the small momentum transfer can be allowed to excite a "plasmon." In a small-k region $|Z_1-\rho_i(k)|^2$ is nearly equal to $(Z_1-1)^2$ where a He^+ ion behaves as a proton. There exists, however, the clear difference in the contribution from the pair excitation branch. The period of the oscillation and the structure of the total stopping power for a He^+ ion seems to be as a proton except for the magnitude of the values. A major portion of the stopping power arises from the pair excitation branch at this energy. These features are common to the cases of 200-, 250-, and 400-keV/amu energies, while the amplitude of the Z_2 oscillation is enhanced with the decrease of the incident ion energy.

In Fig. 3 the calculated ratio of the total stopping power for a He^+ ion, S_{He^+}, to that for a proton, S_{H^+}, are shown at 200, 250, and 400 keV/amu. The existence of the Z_2 oscillation can be notified here, where S_{He^+}/S_{H^+} is enhanced with the increase of the energy and the oscillation amplitude tends to decrease with Z_2. In the atomic picture the maximum ratios are given at the closed-shell-configuration materials. On the other hand, in the solid picture the calculated ratio gives the larger values than in the atomic picture at any energies considered. The fact that S_{He^+}/S_{H^+} is greater than unity without respect to Z_2 is the reason why the effective charge presents a ten-

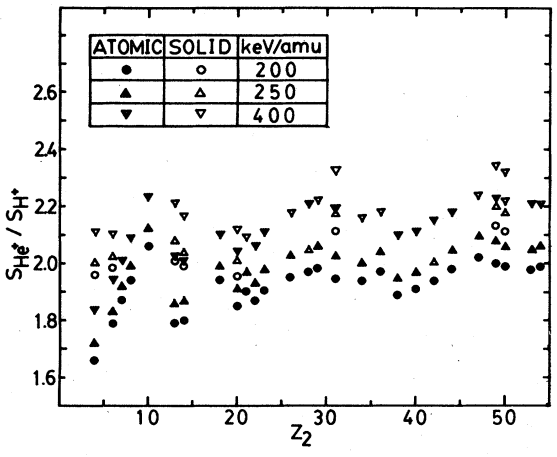

FIG. 3. Theoretical ratio S_{He^+}/S_{H^+} with respect to Z_2 at 200, 250, and 400 keV/amu in the atomic picture and in the solid picture.

dency to depend on Z_2 more weakly than the mean charge, as is seen later.

By using the charge-state fractions of the emerging ions with the calculated S_{He^+} and $S_{He^{2+}}$ $(=2^2 S_{H^+})$ values, the Z_2 dependence of the stopping power for a 1-MeV helium-ion beam is shown in Fig. 4. Though there exists at most about 20% deviation, the overall feature of the calculated values is consistent with the experimental values.[7,25] This deviation is mainly due to the underestimation of the theoretical S_{H^+} values (and consequently

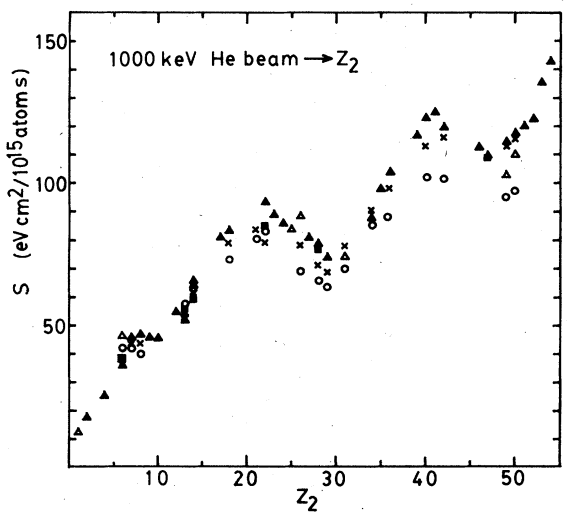

FIG. 4. Z_2 dependence of the electronic stoppping power S_{He} for 250-keV/amu helium-ion beams. The calculated results in the atomic picture and in the solid picture are denoted by (○) and (▲), respectively. The experimental results are in the references: △, Ref. 7; and ■, Ref. 25. The crosses (×) denote the calculated S_{He} values with the use of both the empirical values for S_{H^+} (in Ref. 7) and the theoretical values for S_{He^+}/S_{H^+} in the atomic picture. The charge-state fractions for 250-keV/amu helium-ion beams are cited in Refs. 9, 11, and 12.

$S_{He^{2+}}$), especially at greater Z_2 than 40. This trend has already appeared in Ref. 8, where the calculated stopping power for 1-MeV helium ion became lower than the experimental data in spite of taking the upper-bound charge $Z_1=2$. To improve this situation, a simple prescription is proposed where the empirical S_{H^+} value is substituted for the theoretical one at each Z_2 number with preserving the theoretical ratio S_{He^+}/S_{H^+}. This implies that the better agreement with the experimental S_{H^+} data a theory gives, the better it can be fitted to the experimental data of the stopping power for helium-ion beams.

In Figs. 5(a)—5(c), the theoretical results of the effective charge q_{eff}^{He} are shown with the experimental data obtained by the square root of the ratio of the measured stopping power for helium-ion beams to that for a proton beams at 200, 250, and 400 keV/amu. It is assumed that a proton is bare during its passage in obtaining the experimental q_{eff}^{He}. Since there are more than two data combinations, several points at the same materials are plotted. It should be mentioned that in the lowest figure (400-keV/amu case), q_{eff}^{He} is calculated by using the mean charge $\bar{q}$ mea-

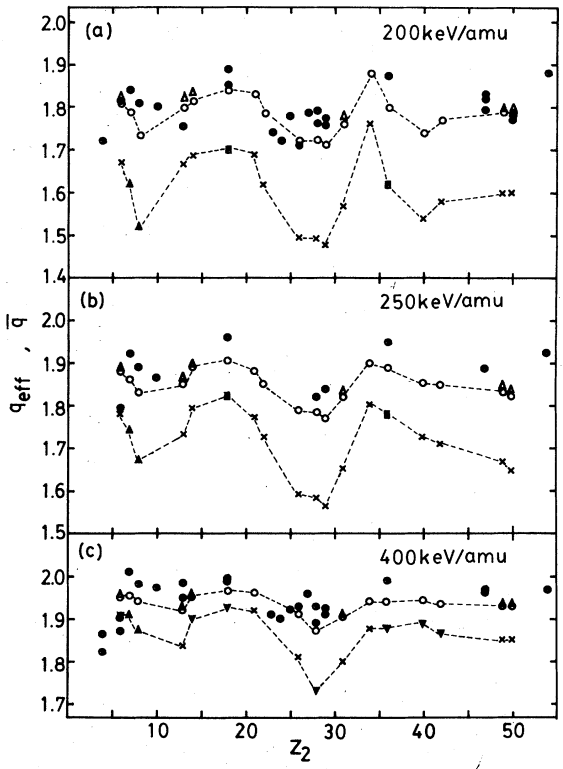

FIG. 5. (a)—(c) Z_2 dependence of the effective charge q_{eff}^{He} for 200, 250, and 400 keV/amu helium-ion beams. Theoretical results are denoted by (— — —○— — —) in the atomic picture and (△) in the solid picture. Experimental plots (●) are obtained by taking the square root of the ratio of the measured stopping power for a helium-ion beam (Refs. 7 and 25) to that for a proton beam (Refs. 19—24) at the same energies. The mean charge $\bar{q}$ for 200-, 250-, and 400-keV/amu helium-ion beams are indicated in the following: ×, Ref. 9; ■, Ref. 11; and ▲, Ref. 12. The symbols (▼) indicate the substitution of the experimental $\bar{q}$ values at 375 keV/amu for those at 400 keV/amu.

sured at 375 keV/amu for C, Si, Ar, Cu, Kr, Zr, and Mo targets. However, since there is, at most, a 2% difference in $\bar{q}$ between 375 and at 400 keV/amu, only a 1% difference in $q_{\text{eff}}^{\text{He}}$ can be actually yielded. The results in Fig. 5 indicate two remarkable features. One is that the calculated $q_{\text{eff}}^{\text{He}}$ values are greater than $\bar{q}$ values at any Z_2 number, and the other is that the Z_2 oscillation of $q_{\text{eff}}^{\text{He}}$ has a smaller amplitude than that of $\bar{q}$. These points are consistent with the experimental results. The first feature $q_{\text{eff}}^{\text{He}} > \bar{q}$ is reasonably understood as follows: for He^{2+} ions, $S_{He^{2+}} = 2^2 S_{H^+}$. Moreover, the relation of the charge distribution of the bound electron in a He^{2+} ion in the Fourier space such as

$$|Z_1 - \rho_i(k)|^2 > |Z_1 - \rho_i(0)|^2 \ (=1)$$

enables us to show $S_{He^+} > S_{H^+}$ as shown in Fig. 3. Therefore we can easily see the following:

$$q_{\text{eff}}^{\text{He}} = (\phi_{He^+} S_{He^+}/S_{H^+} + 2^2 \phi_{He^{2+}})^{1/2} > (\phi_{He^+} + 2^2 \phi_{He^{2+}})^{1/2} > \bar{q} \ . \quad (14)$$

The Z_2 dependence of S_{He^+}/S_{H^+} in contrast with that of $\bar{q}$ weakens strongly the Z_2 dependence of $q_{\text{eff}}^{\text{He}}$. This situation recommends that one assume $q_{\text{eff}}^{\text{He}}$ is constant without regard to Z_2.

The local-density model in the solid picture improves the stopping power values considerably in the high-Z_2 region. Nevertheless, this picture does not increase the magnitude of the effective charge so much. The difference in $q_{\text{eff}}^{\text{He}}$ between two pictures tends to decrease with the increase of the ion velocity. Consequently, the screening effect does not change the calculated $q_{\text{eff}}^{\text{He}}$ so drastically from the results in the atomic picture. Finally it is marked that if the neutral-charge component in the $Z_1 = 1$ beam is included into calculation, the effective charge of the helium-ion beams becomes a little bit greater than the presented results. Actually a few percent of the detected beams are neutral even in the solid targets. For example, hydrogen atoms occupy 4.6%, 1.6%, and 0.5% at 198, 298, and 397 keV/amu, respectively.[26] If these fractions exist in matter, they should be included. It is added here that the neutral-charge component of helium, He^0, can be neglected at the considered energies.

IV. CONCLUSIONS

The paper treated the problem of how the stopping power and the charge states of ion beams in matter could be reconciled for mega-electron-volt helium-ion beams. The charge-state fractions in matter play an important role in determining the stopping power. To include the Z_2 oscillation of the mean charge into the stopping did not change the phase of a well-known Z_2 oscillation in the stopping power for helium-ion beams appreciably. In contrast with a strong Z_2 oscillation in the mean charge, the effective charge did not show so strongly the oscillatory Z_2 dependence, where the amplitude of the oscillation in $q_{\text{eff}}^{\text{He}}$ is smaller than in $\bar{q}$ and the calculated $q_{\text{eff}}^{\text{He}}$ values are always greater than $\bar{q}$ values for the same target regardless of Z_2. They are in good agreement with the experimental results. This is due to the behavior of S_{He^+}/S_{H^+} with respect to Z_2. This Z_2 dependence tends to wipe out the Z_2 dependence of $\bar{q}$. If we do not take into account the size of a partially-stripped ion the effective charge exactly corresponds to the mean charge regardless of Z_2 because of $S_{He^+}/S_{H^+} = 1$. The screening effect in the solid picture yields greater stopping-power values mainly in high-Z_2 region that in the atomic picture. This is partly due to a strong screening condition. Nevertheless this does not affect the magnitude of $q_{\text{eff}}^{\text{He}}$ very much and consequently does not change the Z_2 dependence of $q_{\text{eff}}^{\text{He}}$ drastically. The exit-surface effect will be important in the case of the lower-energy particles emerging from solids. In our case this is not taken into account. With the increase of the ion velocity the interaction time between the ion and the exit surface will decrease and hydrogen atoms cannot be incorporated in the beam. As a result, to include the hydrogen component and the exit-surface effect in $q_{\text{eff}}^{\text{He}}$ in the considered velocity range here will amount to a few percent increase at most. The problem that needs further consideration is how to apply the solid picture to such solids that have too complicated profiles of the energy loss to define the plasma frequency well. To describe the local-electron density for such solids as precisely as possible and, if possible, in a simple form, is a task for the future. If we make an effort to understand not only the target dependence of the stopping power but also that of the effective charge, we have to start with Eq. (1).

ACKNOWLEDGMENTS

This work was financially supported by a Grant-in-Aid for Fundamental Scientific Research from the Ministry of Education, Japan.

[1]As for a helium beam, J. F. Ziegler, in *The Stopping and Ranges of Ions in Matter*, edited by J. F. Ziegler (Pergamon, New York, 1977), Vol. 4.

[2]H.-D. Betz, Rev. Mod. Phys. **44**, 465 (1972).

[3]H. A. Bethe, Ann. Phys. (Leipzig) **5**, 325 (1930).

[4]F. Bloch, Ann. Phys. (Leipzig) **16**, 285 (1933).

[5]J. Lindhard and A. Winther, K. Dan. Vidensk. Selsk. Mat.-Fys. Medd. **34**, No. 4 (1964).

[6]I. Gertner, M. Meron, and B. Rosner, Phys. Rev. A **21**, 1191 (1980).

[7]J. F. Ziegler and W. K. Chu, At. Data Nucl. Data Tables **13**, 463 (1974).

[8]B. M. Latta and P. J. Scanlon, Phys. Rev. A **12**, 34 (1975).

[9]Y. Haruyama, Y. Kanamori, T. Kido, and F. Fukuzawa, J. Phys. B **15**, 779 (1982); Y. Haruyama, Y. Kanamori, T. Kido, A. Itoh, and F. Fukuzawa, *ibid.* **16**, 1225 (1983).

[10]T. Kaneko and Y. H. Ohtsuki, Phys. Status Solidi B **111**, 491 (1982).
[11]L. I. Pivovar, V. M. Tubaev, and M. T. Novikov, Zh. Eksp. Teor. Fiz. **41**, 26 (1961) [Sov. Phys.—JETP **14**, 20 (1962)].
[12]A. Itoh, Ph.D. thesis, Kyoto University, 1979 (unpublished).
[13]W. Brandt and M. Kitagawa, Phys. Rev. B **25**, 5631 (1982); B. S. Yarlagadda, J. E. Robinson, and W. Brandt, *ibid.* **17**, 3473 (1978).
[14]T. Kaneko and Y. Yamamura, Phys. Lett. **100A**, 313 (1984). While the theory is valid, the experimental data in Fig. 1 are drawn a bit mistakenly. The input data of capture and loss cross sections are dictated reversely.
[15]T. L. Ferrell and R. H. Ritchie, Phys. Rev. B **16**, 115 (1977); the extension of the Bethe theory for partially-stripped ions was presented in the following: Y. K. Kim and K. Cheng, Phys. Rev. A **22**, 61 (1980).
[16]T. Kaneko, Radiat. Eff. **70**, 301 (1983).
[17]W. Brandt, in *Atomic Collisions in Solids,* edited by S. Datz, B. R. Appleton, and C. D. Moak (Plenum, New York, 1975), Vol. 1, p. 261.
[18]M. C. Cross, Phys. Rev. B **15**, 602 (1977).
[19]P. K. Weyl, Phys. Rev. **91**, 289 (1953).
[20]M. Bader, R. E. Pixley, F. S. Mozer, and W. Whaling, Phys. Rev. **103**, 32 (1956).
[21]A. Valenzuela, W. Meckbach, A. J. Kestelman, and J. C. Eckardt, Phys. Rev. B **6**, 95 (1972).
[22]H. K. Reynolds, D. N. F. Dunbar, W. A. Wenzel, and W. Whaling, Phys. Rev. **92**, 742 (1953).
[23]J. C. Eckardt, Phys. Rev. A **18**, 426 (1978).
[24]H. Knudsen, H. H. Andersen, and V. Martini, Nucl. Instrum. Methods **168**, 41 (1980).
[25]D. C. Santry and R. D. Werner, Nucl. Instrum. Methods **178**, 523 (1980); *ibid.* **178**, 531 (1980).
[26]S. K. Allison and S. D. Warshaw, Rev. Mod. Phys. **25**, 779 (1953).